

Bakhmutov Vladimir (Orcid ID: 0000-0002-5011-0385)

1

Elucidating Structure and Dynamics of Crystalline α -Zirconium Phosphates Intercalated with Water and Methanol by Multinuclear Solid-State MAS NMR: A Comprehensive NMR Approach.

Vladimir I. Bakhmutov,¹ Aida Contreras-Ramirez,¹ Hannah Drake,¹ and Hong-Cai Zhou^{1,2}

¹ Department of Chemistry, Texas A&M University, College Station, TX 77843, United States

² Department of Materials Science and Engineering, Texas A&M University, College Station, Texas 77843-3003, United States

Correspondence

Vladimir I. Bakhmutov, Department of Chemistry, Texas A&M University, College Station, TX 77842-3012, P.O. Box 30012, United States, Email: bakhmoutov@tamu.edu

Hong-Cai Zhou, Department of Chemistry, Texas A&M University, College Station, TX 77842-3012, P.O. Box 30012, United States, Email: zhou@chem.tamu.edu

Funding information

The U.S. Department of Energy (DOE), Basic Energy Sciences, Grant DE-SC0017864, the Robert A. Welch Foundation (A-0030).

Abstract

Solid-state NMR experiments on ^2H , ^{31}P , ^{13}C and ^1H nuclei, including ^{31}P T_1 , ^1H T_1 , and ^1H $T_{1\rho}$ measurements, as well as on the kinetics of proton-phosphorus cross-polarization have been performed to characterize the crystalline and amorphous α -zirconium phosphates, that were intercalated with D_2O and/or CD_3OD . The $^{13}\text{C}\{^1\text{H}\}$ CP MAS NMR experiment performed for compound **1- CD_3OD** ($\text{Zr}(\text{HPO}_4)_2 \cdot 0.2\text{CD}_3\text{OD}$) with carbon cross-polarization via protons of phosphate groups has provided a prove that the methanol was intercalated into the interlayer spaces of this compound. The variable-temperature ^2H solid-echo MAS NMR spectra of intercalated compounds demonstrated that the methanol molecules, in contrast to the mobile water, were immobile, keeping, however, free CD_3 rotations around the C_3 -axis. It has been demonstrated that the intercalated species, D_2O and CD_3OD , do not affect the high-frequency motions of the phosphate groups. By utilizing local structural models that satisfy the constraints of the experimental data, it has been suggested that the immobile methanol molecules are located in the cavity between two neighboring layers of the zirconium phosphates. Thus, the present work illustrates the reliable criteria in a comprehensive NMR approach to structural and dynamic studies of such systems.

This is the author manuscript accepted for publication and has undergone full peer review but has not been through the copyediting, typesetting, pagination and proofreading process, which may lead to differences between this version and the Version of Record. Please cite this article as doi: [10.1002/mrc.5262](https://doi.org/10.1002/mrc.5262)

KEYWORDS

Zirconium phosphates, solid-state ^2H and ^{31}P NMR, ^1H , ^{31}P relaxation, kinetics of cross-polarization, isotopic exchanges, structural elucidation

1. INTRODUCTION

The extensive studies of layered α -zirconium phosphates, (α -ZrP),^[1-7] have resulted in a wide range usability for these materials in practical applications, including ion exchangers, biosensors, fuel cells, and catalysts. In development of this field, new and important properties of α -ZrP have been discovered due to their intercalation with various inorganic/organic species leading to the creation of molecular systems capable of drug delivery.^[4-6,8] In general, the sphere of practical applications of α -ZrP materials is determined by their structure. However, as it was reported for zirconium phosphate $\text{Zr}(\text{HPO}_4)_2 \cdot \text{H}_2\text{O}$ (**1**),^[9] the structures of these materials can change, ranging from fully-ordered highly-crystalline systems to amorphous and turbostratically disordered layers, depending on methods of their preparations. This situation can be even more complex, when zirconium phosphates are intercalated by different species where both the dynamics and bonding modes of the intercalates play a very important role in structure design. In addition, intercalated species can also effect the motions of the functional groups in the matrix, leading to changes in the properties of the materials. Up to now, however, these aspects are not well studied and have great potential to impact future research directions in this field.

Although there are numerous physical methods applied for the characterization of the different phosphates, solid-state ^{31}P NMR is perhaps the most popular.^[10-11] This technique is

particularly useful for studies of intercalated phosphates,^[12] where the behavior of deuterated guests can be well characterized by experiments on the ²H nuclei.^[13-16] Recently, by conducting ²H and ³¹P{¹H} solid-state MAS NMR experiments on a crystalline layered α -zirconium phosphate system, Zr(HPO₄)₂ • 0.35 D₂O (**1-D₂O**), including ³¹P and ²H T₁ measurements,^[17] it has been revealed that there exists an unusual dynamic/bonding mode of the water, which is hydrogen bonded to the zirconium-coordinated oxygen and experiences a fast rotation (on the time scale of the NMR Larmor frequency) around this bond (Figure 1). At temperatures > 253 K, the intercalated water unprecedentedly shows two spectrally-distinguished deuterons.

Here Figure 1

In a continuation of this work, we report here a full study using ³¹P, ²H, ¹H, and ¹³C solid-state MAS NMR techniques for the comprehensive characterizations of crystalline compounds **1-D₂O-CD₃OD** and **1-CD₃OD** (Table 1), intercalated by water and/or methanol. As earlier, the choice of D₂O is explained by the fact that the water is an important structural element of the α -zirconium phosphates.^[18,19] The interest in utilizing methanol in our work is caused by the well-known catalytic activity of zirconium phosphates in the practically important decomposition of the alcohols.^[20] In addition to the crystalline systems, we have also studied the amorphous compounds including the intercalated and anhydrous α -ZrP variants (Table 1) determining, thus, the reliable criteria in a comprehensive NMR approach to structural and dynamic studies of such systems.

Table 1. The α -ZrP phosphates investigated in the present work.

Compound	Formulation*	Texture
----------	--------------	---------

1	Zr(HPO ₄) ₂ ·H ₂ O	Crystalline
1-An	Zr(HPO ₄) ₂	Crystalline
1-An-Am	Zr(HPO ₄) ₂	Amorphous
1-D₂O	Zr(HPO ₄) ₂ ·0.35D ₂ O	Crystalline
1-D₂O-Am	Zr(HPO ₄) ₂ ·0.5D ₂ O	Amorphous
1-D₂O-CD₃OD	Zr(HPO ₄) ₂ ·0.4D ₂ O·0.2CD ₃ OD	Crystalline
1-CD₃OD	Zr(HPO ₄) ₂ ·0.2CD ₃ OD	Crystalline

* Since the ³¹P MAS NMR spectra show from one to three phosphorus signals for the phosphate groups neighboring with water or methanol molecules or in the absence of both molecules, these signals can be integrated by their deconvolution to obtain the ratio of Zr(HPO₄)₂ to Zr(HPO₄)₂ • D₂O (or Zr(HPO₄)₂ to Zr(HPO₄)₂ • CD₃OD) fragments. Here we consider a content of one water molecule (or one methanol molecule) neighboring with the structural Zr(HPO₄)₂ fragment as maximal one, providing, thus, a semi quantitative formulation.

2. EXPERIMENTAL

2.1. Materials. Initial crystalline compound **1** was prepared with a concentrated phosphoric acid (~14.7M), according to the previously described method.^[9] A sample of this compound (as well as other samples) was dried at 100 °C for 24 hrs in a well-packed NMR rotor placed into a petri dish which was located in an oven to obtain a white powder of anhydrous crystalline zirconium phosphate **1-An**. Then, a sample of **1-An** was poured into a glass vial and soaked with methanol-d₄ (Sigma-Aldrich) for 30-40 min in proportion of ~ 1g of **1-An** and 5 mL of CD₃OD. The sample was then placed into an oven at 100°C for 10 -15 min to remove the excess liquid component, as monitored by ²H MAS NMR. Then, using the same procedure, samples of the resulting product were soaked with D₂O (Sigma-Aldrich) for 2 h to obtain compound **1-D₂O-CD₃OD**. After removing the liquid components, deconvolution as performed for the phosphorus resonances in the ³¹P{¹H} MAS NMR spectra leads to the formulation of these compounds as in Table 1.

Compound **1-CD₃OD** was similarly prepared from crystalline **1-An** soaked in methanol-d₄ only. The crystalline compound **1-D₂O** was prepared as previously described in the literature.^[17] The amorphous compound of **1-D₂O-Am** formulated in Table 1 on the base of ³¹P{¹H} MAS NMR, was obtained from amorphous material **α-ZrP**⁹ by treatment with D₂O and dried under vacuum at 295 K for 30 min to eliminate the excess liquid component. To obtain the amorphous compound **1-An-Am**, compound **1-D₂O-Am** was fully dried at 100 °C in an oven.

2.2. NMR Techniques and Measurements. The ³¹P{¹H}, ¹³C{¹H}, ¹H and ²H MAS NMR experiments were carried out with a Bruker Avance-400 solid-state NMR spectrometer (400 MHz for ¹H nuclei) equipped with a standard two-channel 4-mm MAS probe head. The external standards, used for ¹³C, ²H, and ³¹P NMR were referenced to TMS and (NH₄)₂HPO₄, respectively.

The standard single pulse (direct nuclear excitation) and/or cross polarization (CP) pulse sequences were applied for both ³¹P and ¹³C nuclei at time delays needed for the full spin–lattice relaxation. The contact times of 5 ms and 6 ms were adjusted for the ¹³C and ³¹P nuclei, respectively, to observe the regular proton-carbon and proton-phosphorus CP MAS NMR spectra. ³¹P CSA values were obtained through the full data analysis of the NMR spectra with a standard Bruker program package exemplified in Figure S1.

The ³¹P{¹H} CP MAS NMR experiments including the ¹H spin-lock sections were carried out with a standard Bruker pulse sequence, cphT1rho, with H-P CP contact times of 5 ms. For each sample, the single-scan ³¹P{¹H} CP MAS NMR experiments have been performed with a proton

locking time of 0.1 μs and 16000 μs at a ^1H power of 50 w to compare the corresponding signal intensities.

As the ^{31}P T_1 times measured for the crystalline compounds investigated in the present work are quite long, all the $^{31}\text{P}\{^1\text{H}\}$ MAS NMR spectra were obtained with one or two scans. The room-temperature ^{31}P T_1 relaxation measurements were performed through standard inversion–recovery ($180^\circ\text{--}\tau\text{--}90^\circ$) experiments with the well calibrated *rf* pulses on the samples spinning at a rate of 7 and 10 kHz. Relaxation (recycle) delays were adjusted to provide full nuclear relaxation. The experimental inversion–recovery curves “signal intensity versus τ time” have been treated with a standard nonlinear fitting computer program based on the Levenberg–Marquardt algorithm. ^1H T_1 times were also measured by inversion–recovery experiments.

^2H MAS NMR spectra were recorded with a regular solid-echo pulse sequence with a 90° *rf* pulse of 3.5 μs and recycling delays of 2.5 s an account for the ^2H T_1 time estimated for the CD_3 groups in compound **1- CD_3OD** as ~ 0.5 s. DQCC calculations were carried out by a sideband analysis with a standard Bruker program package.

The kinetics of the proton-phosphorus cross-polarization were studied by variations in the contact times between 25 100 and 10 000 μs used for the $^{31}\text{P}\{^1\text{H}\}$ CP MAS NMR experiments. The kinetic data was treated with a standard fitting computer procedure.

The variable- temperature MAS NMR experiments have been performed with a standard temperature unite of the spectrometer. Temperature corrections for spinning samples did not carry out.

2.3. The X-Ray Diffraction. Powder X-Ray Diffraction (PXRD) patterns were obtained with a Bruker-AXS D8 short arm diffractometer equipped with a multiwire lynx eye detector using Cu ($K\alpha$, $\lambda=1.542\text{\AA}$). It was operated at a potential of 40 kV and a current of 40 mA. The software suit for data collection and evaluation is windows based. Data collection is automated COMMANDER program by employing a DQL file. Data is analyzed by the program EVA.

2.4. EPR. The data were collected with a Bruker ELEXSYS II E 500 spectrometer operating at 9.75 GHz (X-band) and using the Xepr software.

The collected PXRD patterns and some additional MAS NMR spectra are placed in Supplementary Information.

3. RESULTS AND DISCUSSION

3.1 $^{31}\text{P}\{^1\text{H}\}$ MAS NMR. Since the solid-state $^{31}\text{P}\{^1\text{H}\}$ NMR spectra are widely applied for characterization of zirconium phosphates,^[18,21] in this section we discuss the $^{31}\text{P}\{^1\text{H}\}$ MAS NMR experiments performed on samples of the crystalline intercalated and anhydrous phosphates **1-D₂O-CD₃OD**, **1-CD₃OD** and **1-An**.

The $^{31}\text{P}\{^1\text{H}\}$ MAS NMR spectrum of crystalline compound **1-D₂O-CD₃OD**, obtained with direct excitation of ^{31}P nuclei, is shown in Figure 2A, where we observed three differently-intense

Here Figure 2

phosphorus resonances, belonging to the structurally-distinguished HPO_4 groups. Since the chemical shift differences for these resonances, as in the case of compound **1-D₂O**,¹⁷ are quite

small ($\delta(\text{iso}) = -21.0, -23.0$ and -24.5 ppm), their accurate assignment is questionable and requires additional data and processing.

As follows from Figure 2A, the low-field resonance of compound **1-D₂O-CD₃OD** with the chemical shift $\delta(\text{iso})$ of -21.0 ppm was shown to grow after an additional treatment of this compound by D₂O. This effect was also accompanied by decreasing the signal at $\delta(\text{iso})$ of -24.5 ppm, belonging to HPO₄ neighboring with CD₃OD (see below) due to partial replacement of the methanol by the water. In turn, the resonance at $\delta(\text{iso})$ of -21.0 ppm, practically invisible in the ³¹P{¹H} MAS NMR spectrum of the anhydrous compound **1-An** developed again when the anhydrous compound **1-An** was treated with H₂O or D₂O. Such a reversible spectral behavior of the low-field signal corresponds well to the HPO₄ groups neighboring with water molecules. This agrees well with the reported literature.^[17] A resonance at $\delta(\text{iso})$ of -23 ppm observed in the spectrum of crystalline compounds **1-D₂O-CD₃OD** and **1-An** was assigned to the “water-free” HPO₄ groups; again in agreement with reported literature.^[17] Finally, the third resonance at $\delta(\text{iso})$ of -24.5 ppm, appearing only in the presence of methanol, was assigned to HPO₄ groups experiencing influence of the CD₃OD molecules. It should be noted that observations of the HPO₄ groups neighboring with the methanol at the highest magnetic field ($\delta = -24.5$ ppm) could be attributed to an acceptor hydrogen bond P-(H)O⋯DOCD₃ formed by interlayer phosphate groups.^[21] However, such a bonding could reduce the high-frequency mobility of the phosphate groups which, however, does not change in the presence of the methanol (see below). Therefore,

hydrogen bonding to a zirconium-coordinated oxygen, similarly to the water^[17] in Figure 1, is more preferable.

An important element in this section is the fact that all three resonances of compound **1-D₂O-CD₃OD** demonstrate the equal effectiveness of the *proton*-phosphorus cross-polarization^[22] (Figure 2B) in spite of the structural difference of the HPO₄ groups. This result is possible when H···P distances, number of closest proton neighbors with phosphorus atoms (one proton in the case of the compounds), and the mobility are identical for these phosphate groups.^[22] Finally, the minor signal in the ³¹P{¹H} MAS NMR spectrum of anhydrous (fully-dried) compound **1-An**, situated in the zone of the chemical shifts for α-ZrP,^[21] is difficult to assign accurately. Since the ²H MAS NMR spectrum of **1-An** does not show the resonances of D₂O, this minor phosphorus resonance with the chemical shift, corresponding to HPO₄ groups, neighboring with water, can potentially appear due to H₂O absorbed on the surface by the material during manipulations with the samples. Due to its small intensity, it will be not considered later on.

The ³¹P{¹H} MAS NMR spectra in Figure 2, themselves, do not prove that the methanol molecules are actually intercalated into interlayer spaces. The proof of the intercalation comes from the ¹³C{¹H} CP MAS NMR experiment which was carried out for a sample of crystalline compound **1-CD₃OD**. As seen in Figure 3, the ¹³C{¹H} CP MAS NMR spectrum shows the ¹³CD₃ resonance

Here Figure 3

of the methanol. This signal, detected via the *proton-carbon cross-polarization* could only be observed at the close location of the CD₃ groups to the protons in the phosphate groups. It should be emphasized that the molecules on the surface generally experience fast isotropic reorientations. Under this condition cross-polarization will be not possible. In addition, the ¹³CD₃ resonance in compound **1-CD₃OD** was low-field shifted to a δ(iso) of 52.2 ppm versus the 49.0 ppm chemical shift of liquid methanol.

According to the structural PXRD characterization,^[9] compound **1-D₂O** prepared through the treatment of crystalline compound **1** by D₂O remains crystalline and layered with the interlayer distance of 7.6 Å.^[17] As seen in Figure 2, the linewidths of the phosphorus resonances in the ³¹P{¹H} MAS NMR spectra do not practically change at manipulations with compound **1-D₂O-CD₃OD**. The PXRD pattern of this intercalated compound exhibited two peaks corresponding to two types of layers at distances 8.6 and 7.6 Å (Figure S2), where slight increasing the interatomic distance to 8.6 Å is caused probably by the intercalation. In accord, only one type of interlayer distance, 7.6 Å, is observed in PXRD pattern of the anhydrous compound **1-An**, after elimination of the intercalates (Figure S2). Independently structural ordering and homogeneity of compounds **1-D₂O-CD₃OD** and **1-An** can be verified by ³¹P{¹H} CP MAS NMR experiments carried out with pulse sequences including a ¹H spin-lock section. Note that this experimental strategy, being standard to estimate contents of the ordered and disordered phases, has been successfully applied for characterizations of different crystalline and amorphous zirconium phosphates.^[9] In accord to the generally-accepted protocol,^[23] in the presence of the ¹H spin-lock section, high-ordered phases

can be detected while the disordered (amorphous) phase can be estimated by the corresponding spectral difference. As follows from the spectral data presented in Figure S3, the disordered phase in compounds **1-D₂O-CD₃OD** and **1-An** does not exceed 5-7%. In contrast, the same $^{31}\text{P}\{^1\text{H}\}$ CP MAS NMR experiments, performed for compound **1-D₂O-Am** prepared from amorphous material $\alpha\text{-ZrP}$,^[9] reveals a disordered phase of 36-38%. Thus, as in the case of **1-D₂O**,^[17] at the preparation of compound **1-D₂O-CD₃OD** and subsequent experimental manipulations with the samples to obtain compound **1-An**, the structures of the phosphates maintain their crystallinity. This result is very valuable for the interpretations of the ^{31}P T_1 time measurements in section *^{31}P T_1 Studies*.

To characterize additionally the environment of the ^{31}P nuclei we have measured the ^{31}P chemical shift anisotropy (^{31}P CSA) in anhydrous and intercalated compounds **1-An** and **1-D₂O**. The ^{31}P CSA values were calculated by using the ^{31}P static and MAS NMR experiments, performed at spinning rates of 3 and 4 kHz. The ^{31}P CSA values, obtained at asymmetry parameters η of ≤ 0.3 are: 37 ± 4 ppm for the resonance with $\delta(\text{iso})$ of -23 ppm in compound **1-An** and 30 ± 3 ppm for resonances at $\delta(\text{iso})$ of -21 ppm and $\delta(\text{iso})$ of -23 ppm in compound **1-D₂O**. As seen, the compounds show relatively low ^{31}P CSA values close to that in amorphous $\alpha\text{-ZrP}$ (34.5 ppm^[24]), which can be associated with a practically symmetric local environment in the PO_4 fragments.

3.2. The Proton-Phosphorus Cross-Polarization $^{31}\text{P}\{^1\text{H}\}$ MAS NMR Experiments. Besides the regular $^{31}\text{P}\{^1\text{H}\}$ MAS NMR experiments, the spectrally-distinguished phosphate groups in the crystalline intercalated compounds **1-D₂O-CD₃OD** and **1-CD₃OD** and also the phosphate groups in anhydrous compound **1-An** were characterized by experiments on the kinetics of proton-

phosphorus cross-polarization.^[22] These experiments are important in the context of understanding structures of the phosphate compounds investigated in the present work.

The cross-polarization experiments, which were varied in contact times, are shown in Figure 4 with compound **1-D₂O-CD₃OD** as an example. Since the collected data do not show the oscillations typical of a I-I*-S cross-polarization model even at shortest CP times of 25 and 50 μ s, they can be approximated by a classical spin I-S model,^[22] resulting in

Here Figure 4

the determination of the polarization constants, T(H-P), and T_{1p}(¹H) relaxation times in the rotating coordinate system listed in Table 2. Theoretically, the T(H-P) constants depend on three factors: H...P distances, number of closest protons participating in the cross polarization and the mobility of the HPO₄ groups.^[22] Table 2 shows that the T(P-H) constants, obtained for crystalline

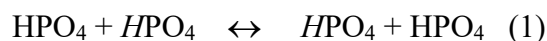
TABLE 2. The cross-polarization constants, T(P-H), and the T_{1p}(¹H) times determined in the rotating coordinate system via the proton-phosphorus cross-polarization kinetics at 295 K.

Compound	/	δ (ppm)	T(P-H) (ms)	T _{1p} (¹ H) (ms)
1-D₂O-CD₃OD	/	-21	0.68 \pm 0.07	54 \pm 7
	/	-23	0.79 \pm 0.08	51 \pm 6
	/	-24.5	0.62 \pm 0.06	52 \pm 6
1-CD₃OD	/	-23	0.72 \pm 0.07	-
	/	-24.5	0.66 \pm 0.07	-
1-An	/	-23	0.53 \pm 0.05	53 \pm 6
1-An-Am	/	-22.5	0.54 \pm 0.05	31 \pm 7

compounds **1-D₂O-CD₃OD** and **1-CD₃OD** are almost equal. Since it is difficult to expect a mutual compensating effect for all of three factors, which makes the T(P-H) constants equal for the structurally-different phosphate groups, the behavior of these groups in the CP experiments is rather identical in spite of the presence of intercalated neighbors. It is also remarkable that the amorphous (**1-An-Am**) and crystalline (**1-An**) anhydrous compounds show practically the same T(P-H) constants of 0.54 and 0.53 ms, respectively.

In addition to the cross-polarization constants, Table 2 lists the $T_{1\rho}(^1\text{H})$ times characterizing the protons that are involved into the cross polarization. Since these values were obtained by the calculations of the corresponding CP curves, accuracy of their determinations is not high. In addition, due to a long $T_{1\rho}(^1\text{H})$ time,^[22] the character of the CP curve, presented in Figure S4, did not allow to obtain this parameter for compound **1-CD₃OD**. The $T_{1\rho}(^1\text{H})$ relaxation in solids is governed by magnetic field fluctuations caused by proton motions on the low frequency scale. However due to the presence of ^1H spin diffusion, the relationship between the relaxation times and motions is not straightforward.^[22] Nevertheless, the ^1H $T_{1\rho}(^1\text{H})$ times remains an important parameter for characterization of different molecular systems. In contrast to the $T_1(^1\text{H})$ time, the $T_{1\rho}(^1\text{H})$ time in the rotating coordinate system is associated with a low-frequency motion, recognized earlier for zirconium phosphate **1**, as a proton transfer between phosphate groups.^[24] As it has been reported, the $T_{1\rho}(^1\text{H})$ time of 51 ms characterizes this proton transfer at 295 K as fast on the T_2 NMR time scale with a correlation time of 1.5×10^{-5} s. Since the $T_{1\rho}(^1\text{H})$ times presented in Table 2 for crystalline compounds **1-D₂O-CD₃OD** and **1-An** show the same values,

the fast proton transfer can be postulated for these compounds. Note that the proton transfer should lead to the proton-proton exchange shown in eq. (1) which, in turn, can occur through hydrogen bonds formed by the phosphate groups as shown in Figure 1.



According to the principles of NMR, due to the fast proton-proton exchange between the phosphate groups, the HPO₄ groups observed in ³¹P{¹H} MAS NMR spectra as spectroscopically-distinguished will be equivalent in the ¹H MAS NMR spectra. This effect is illustrated in Figure S5 where the ¹H MAS NMR spectrum of **1-D₂O** manifests a *single* HPO₄ resonance at δ(iso) ~ 7 ppm, the shape of which does not change in a fully dried sample (see also the comments to Figure S5). Similar behavior of the HPO₄ resonance was found for compound **1-CD₃OD** where the linewidth in the ¹H MAS NMR spectrum did not change with the temperature between 295 and 210 K. Thus these data illustrate experimentally the presence of the fast proton-proton exchange (1).

3.3. ³¹P T₁ Studies. For crystalline compounds **1-D₂O-CD₃OD**, **1-CD₃OD**, and **1-D₂O**^[17] mutual interactions between phosphate groups and intercalates and particularly the influence of intercalated molecules on the high-frequency mobility of the spectroscopically-different HPO₄ are of great interest. The expected influence was probed by measuring the corresponding ³¹P T₁ relaxation times. As the NMR relaxation of the phosphorus nuclei in zirconium phosphates is governed by *proton*-phosphorus dipolar interactions modulated by high-frequency rotations of

HPO₄ groups around the P-O axis,^[24] the ³¹P T₁ relaxation times can be sensitive to the presence of the intercalates.

According to our measurements, demonstrated in Figure 5 with compound **1-D₂O-CD₃OD**

Here Figure 5

as an example, the phosphorus spin-lattice relaxation in the crystalline compounds is close to exponential. In fact, the relaxation curves obtained for **1-D₂O**, **1-D₂O-CD₃OD**, **1-CD₃OD**, and **1-An** and fitted to a stretched exponential, $f(t) = \exp(-t/T_1)^\beta$ give the β values between 1 and 0.75 (Table 3). As noted in the literature, the ³¹P T₁ relaxation times of phosphate groups in solids change in very large limits: from ~100 s in a natural apatite to 4 s in a synthetic apatite, or between 0.8 and 40 s in zirconium phosphates,^[25-27] depending on different factors including the morphology of the materials. The latter factor is reasonable because group reorientations contributing to dipolar relaxation rates are faster in amorphous solids. As seen in Table 3, the ³¹P T₁ times in crystalline compounds **1-D₂O**, **1-D₂O-CD₃OD** and **1-CD₃OD** are extremely long, surpassing all the above mentioned values. In fact, these ³¹P T₁ times are strongly longer than 0.14×10^2 s, reported earlier for the amorphous zirconium phosphate **1**.^[24] At the same time, they differ not so strongly from 1.1×10^2 s, measured in the present work for the especially prepared crystalline phosphate **1**.

TABLE 3. The phosphorus spin-lattice relaxation times, ^{31}P T_1 , obtained with errors $\pm 10\%$, by the inversion-recovery ^{31}P MAS NMR experiments and calculated by a stretched exponential with the corresponding β parameter.

Compound	/ δ (ppm)	^{31}P $T_1 \times 10^2$ (s) / ^{31}P $T_1(50) \times 10^2$ (s)	β
1-D₂O ¹⁷	/ -21	1.9 / 3.0	0.93
	/ -23	2.0 / 3.0	0.99
1-D₂O-CD₃OD	/ -21	2.3 / 3.0	0.70
	/ -23	2.8 / 3.7	0.70
	/ -24.5	2.1 / 3.0	0.80
1-CD₃OD	/ -23	4.0 / 5.4	1.0
	/ -24.5	3.5 / 4.5	0.75
1-An	/ -23	3.4 / 3.8	0.78
1-D₂O-Am	/ -21	0.52 / 0.88	0.58
	/ -23	0.41 / 0.73	0.55
1-An-am	/ -22.5	0.37 / 0.63	0.57

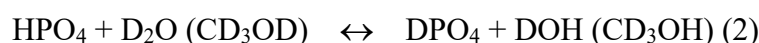
The elongating spin-lattice relaxation time effect is well documented in NMR of different molecular systems in going from disordered to crystalline phases due to decreasing molecular mobility in the crystalline compounds.^[28,29] In addition, at the preparation of amorphous zirconium phosphates, which are often porous, there is a possibility of trace paramagnetic centers accumulated in such samples. For example, paramagnetic metal ions, such as Fe^{+3} , may be present in the sample, accelerating the ^{31}P relaxation.^[24,25] To verify these effects, we have studied the differences between our amorphous compounds **1-D₂O-Am** and **1-An-Am** versus our crystalline compound **1-D₂O**, **1-D₂O-CD₃OD** and **1-CD₃OD**. As noted above, compound **1-D₂O-Am** is

disordered for 36-38%. Table 3 shows that the ^{31}P T_1 times in the amorphous compounds **1-D₂O-Am** and **1-An-Am** are shorter by a factor of ~ 4 . Note also that the phosphorus relaxation in these samples becomes not exponential, showing the lower β values in Table 3. It is remarkable that the same β value (0.56) was reported earlier for amorphous zirconium phosphates,^[24] indicating the consistency of our results with the literature. Since the samples of amorphous compound **1-D₂O-Am** and crystalline compound **1-D₂O** did not manifest any EPR resonances, indicating no paramagnetism in the samples, the elongating ^{31}P T_1 effect in Table 3 can be fully attributed to the crystalline nature of the compounds. In fact, rotations of HPO_4 groups around the P-O axis in crystalline systems can be slower (remaining fast on the Larmor frequency scale), for example, due to a more ordered hydrogen-bond net (Figure 1). It is interesting that the same T_1 tendency is observed for the ^1H T_1 times of HPO_4 groups ($\delta(\text{iso}) \sim 7$ ppm), probed by the ^1H MAS NMR experiments. The values for crystalline compounds **1-D₂O**, **1-An**, and **1-CD₃OD** were measured to be 5.5, 13.6, 12.6 s, respectively, versus 0.18 s in amorphous compound **1-D₂O-Am**.

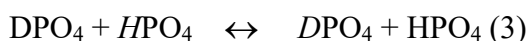
As seen in Table 3, the ^{31}P T_1 times were obtained at different β values. Therefore, their comparison will be corrected by using the parameter $T_1(50)$, which corresponds to a 50% recovery of the signal intensity.^[25] Our results indicate that the ^{31}P $T_1(50)$ times moderately change for compounds **1-D₂O**, **1-D₂O-CD₃OD**, **1-CD₃OD** and **1-An** (between 3×10^2 and 5.4×10^2 s) to show in all cases the *equal* relaxation times for the spectroscopically- and structurally-different HPO_4 groups. Note that the same effect is observed for compound **1-D₂O-Am** in spite of its amorphous

nature. Thus, the presence of the intercalates *does not restrict* the high-frequency HPO_4 motions in the investigated compounds.

One of the important properties of zirconium phosphates is their potential proton conduction, the mechanism of which consists of fast exchanges between the protons of the water molecules on the surface of the layers and the acidic protons of the HPO_4 groups.^[30-33] In terms of such exchanges, the preparation of compounds **1-D₂O**, **1-D₂O-CD₃OD**, and **1-CD₃OD** by treatment of **1** with D_2O and/or CD_3OD could lead to the appearance of DPO_4 groups via *deuterium*-proton exchange (2). In turn, these DPO_4 groups can affect the interpretation



of the experimental data collected in this work, particularly the ^{31}P T_1 times in Table 3. Theoretically, a replacement of a proton for a deuteron in a functional group must reduce the dipolar phosphorus relaxation rate by a factor $(\gamma(\text{H})/\gamma(\text{D}))^2 \sim 40$. However, the ^{31}P inversion-recovery spectra, recorded for the investigated compounds with the pulse sequence 180- τ - 90 at varying time τ between 1000 and 50 s do not reveal the presence of any long-relaxing phosphorus components that could be attributed to DPO_4 groups. The absence of such components agrees with the *proton*-phosphorus cross-relaxation experiments where DPO_4 groups were also not detectible. Note however, that the above-mentioned spectral observations are still possible under conditions of fast (on the T_2 NMR time scale) isotope exchange (3) (equivalent to exchange (1)) between the structurally-different phosphate groups which can lead to a homogeneous



deuterium distribution between them. This is particularly true when the D content is not high. In the frameworks of the considered concept, the fast isotope exchange is capable of averaging ^{31}P OD and ^{31}P OH signals (caused by a secondary isotope chemical shift effect) and their ^{31}P T_1 times for each phosphorus resonance of the spectroscopically-different phosphate groups. Following these statements, one can compare the ^{31}P T_1 time of 1.1×10^2 s, measured for crystalline compound **1** (i.e. in the absence of DPO_4 groups) and the ^{31}P T_1 time of 2.8×10^2 s taken as an averaged relaxation time observed for the crystalline intercalated compounds in Table 3. Then, applying the $(\gamma(\text{H})/\gamma(\text{D}))^2 \sim 40$ factor in equation (4)

$$1/^{31}\text{P}T_1(\text{obs}) = (a) 1/^{31}\text{P}T_1(\text{POH}) + (1-a) 1/^{31}\text{P}T_1(\text{POD}) \quad (4)$$

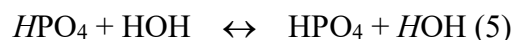
(valid for a fast NMR exchange between the phosphate groups, for example, through H-bonds in Figure 1, where a is the corresponding mole fraction) leads to a DPO_4 content in the intercalated compounds estimated as low as $\leq 4\%$ only. Such a small D content (even if D is present) does not obviously change the main conclusion of this section: the intercalates *do not affect* HPO_4 motions in the investigated materials. Moreover, at this small DPO_4 content, the DPO_4 groups can remain invisible in the ^2H solid-echo MAS NMR spectra as it is observed in section ^2H NMR.

The ^1H T_1 relaxation times, determined for the proton signals in the ^1H MAS NMR spectrum of compound **1-H₂O-Am**, prepared from amorphous material $\alpha\text{-ZrP}$ complete this section characterizing the intercalated water. The $^{31}\text{P}\{^1\text{H}\}$ MAS NMR spectrum of this compound, shown in Figure 6A manifests two resonances at -21 and -23 ppm, which correspond

Here Figure 6

to the structurally-different phosphate groups, noted earlier for compound **1-D₂O**.¹⁷ As earlier, a fully-dried sample of **1-H₂O-Am** shows only one resonance at -23 ppm. In accordance with deconvolution of the phosphorus resonances in the ³¹P {¹H} MAS NMR spectrum, compound **1-H₂O-Am** can be formulated as Zr(HPO₄)₂·0.42H₂O. As seen in Figure 6B, the ¹H MAS NMR spectrum of **1-H₂O-Am** exhibits two relatively sharp resonances (accompanied by spinning site bands) observed at δ(iso) of 8.2 and 3.9 ppm. This is in good agreement with the ²H chemical shifts of the deuterons in the intercalated water and its bonding mode.¹⁷ In addition, a single resonance of HPO₄ groups is observed at δ(iso) = 7.1 ppm due to the *fast H/H exchange* in eq. (1) between the protons of the structurally-different phosphate groups. In addition, an exchange between protons of HPO₄ groups and H₂O is obviously slow on the NMR time scale. It is remarkable that after full drying the water resonances disappear to show only the HPO₄ resonance in the ¹H MAS NMR spectrum (Figure 6B). The inversion-recovery relaxation experiments, characterizing the intercalated water in compound **1-H₂O-Am** at the proton level have led to the ¹H T₁ times of 0.25±0.02 s and 0.28±0.02 s for the water resonances at δ(iso) of 8.2 ppm and 3.9 ppm, respectively. Thus, in contrast to the strongly-different ²H T₁ relaxation times of deuterons in **1-D₂O**,¹⁷ the protons of the intercalated water show the equal ¹H T₁ times. This result strongly supports the bonding/dynamic mode of the water in Figure 1, where the water molecules experience the fast rotation.¹⁷ In fact, the rotating dipolar H-H vector will obviously lead to the identical relaxation of both protons via dipole-dipole proton-proton interactions while deuterons in D₂O relax via quadrupolar interactions. It is interesting that HPO₄ groups in **1-H₂O-Am** relax

faster (the ^1H T_1 time is measured as 0.19 s) than the water protons revealing, thus, the absence of exchange (5) on the NMR time scale.



3.4. ^2H MAS NMR. The dynamic / bonding mode of the intercalated water in the crystalline compound **1-D₂O** (Figure 1) has been established earlier^[17] by the variable-temperature ^2H MAS NMR experiments. The room-temperature ^2H solid-echo MAS NMR spectrum of compound **1-D₂O-CD₃OD**, intercalated by both water and methanol, manifests quadrupolar patterns of D₂O and CD₃OD, a number of which does not allow to calculate the spectrum accurately. Therefore, the intercalated methanol was characterized in crystalline compound **1-CD₃OD**.

The variable-temperature ^2H solid-echo MAS spectra of compound **1-CD₃OD** recorded with the optimized relaxation delays of 3 s are shown in Figure 7, where the highly-

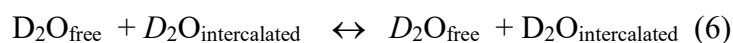
Here Figure 7

intensive quadrupolar pattern evidently belongs to the CD₃ group. This pattern was characterized by chemical shift $\delta(\text{iso})$ of 4.3 ppm, while a *single* low-intensive OD resonance, accompanied by wide spread of spinning sidebands, was observed at $\delta(\text{iso}) = 8.6$ ppm (Figure 7 and Figure S6). As seen, these spectra, like in the case of compound **1-D₂O**^[17] do not manifest DPO₄ groups discussed in the previous sections.

The calculations performed for the ^2H MAS NMR spectrum at 325 K (Figure S6) resulted in two sets of quadrupolar parameters: DQCC of 44 ± 3 kHz ($\eta=0.4$) for the CD₃ groups and DQCC of 195 ± 7 kHz ($\eta=0.1$), corresponding to the OD groups. The DQCC(CD₃) value of 44

kHz is close to that reported for methanol-d₄ molecules located in the pores of MCM-41 at 160 K.^[34] In this instance, the methanol molecular reorientations are fully frozen while the free rotation of the CD₃ groups around the C₃-axis are still active. It is important to note that the DQCC constant of the OD groups is very close to that characterizing the hydrogen-bonded deuteron of water in crystalline D₂O.^[17] Upon cooling to 213 K, the ²H NMR spectrum of compound **1-CD₃OD** changes only slightly (Figure 8) to show the DQCC(CD₃) value of 50±5 kHz. Thus, in contrast to the water in D₂O,^[17] the methanol molecules, intercalated into interlayer spaces of compound **1-CD₃OD** are immobile with the exception of the above-mentioned free CD₃ rotation.

In the context of discussing the ²H NMR experiments performed in the present work, an interesting result was obtained for a sample of compound **1-D₂O**, which after the preparation was shortly placed into an oven at 100 °C for 15 min. The ²H MAS solid-echo NMR spectrum of this sample, presented in Figure S7 manifests an intensive/sharp resonance which can be well assigned to the liquid-like isotropically-moving D₂O. This resonance neighbors with the quadrupolar patterns, belonging to the intercalated water. As all the lines in this spectrum are sharp, a D/D exchange between two different states of water (6) can only be slow on



the T₂ NMR time scale.

Finally, according to the ²H MAS NMR data, collected in the present work, D₂O easily replaces CD₃OD in our compounds but not *vice versa*, while intercalation of CD₃CN, (CD₃)₂CO

and C₆D₆ into crystalline compound **1-An** was unsuccessful. Thus, *donor* H-bonding and the molecular size of the intercalated species play a main role at intercalation.

3.5. Structure Model for Zirconium Phosphates Intercalated with Methanol.

Since the bonding mode and dynamics of the intercalated water in crystalline compound **1-D₂O** is already known^[17] (see Figure 1), in this section we suggest a local structure model for α -zirconium phosphates intercalated with methanol molecules. The structure of the crystalline α -zirconium phosphate is well established (Figure 1). In this structure, there is a layered stacking (7.6 Å apart) which produces a cavity with a diameter of 2.61 Å^[19] sufficient to be occupied by a mobile water molecule.^[17] Since the total molecular volume of the methanol molecule (~ 4Å) is remarkably larger, the cavity volume provides to hold the CD₃ group of the methanol only. This simple consideration along with knowledge gained from our experiments can be used to suggest the local structure of compound **1-CD₃OD**. The experimental results can be summed up as (a) the intercalation of the methanol molecules is achieved by a simple soaking of the compounds that is associated with the accessibility of the free interlayer spaces which are interconnected via micro channels,^[35] (b) the ¹³C{¹H} CP MAS NMR experiment demonstrates close proximity between the phosphate protons and CD₃ groups; (c) the methanol molecules, as well as the water molecules, do not affect the mobility of neighboring phosphate groups; (d) like in zeolites, the methanol intercalated in our structures are capable of forming hydrogen bonds,^[36-38] which in our case are formed by the OD group and the zirconium-coordinated oxygen (as a result, no movements of phosphate groups are obstructed); (e) the methanol molecules are immobile in our structures, with

the exception of the free CD₃ rotation around the C₃-axis. As we believe, the structural model, shown in Figure 8 satisfies

Here Figure 8

all the above factors, where the immobile methanol molecule is locating in two neighboring layers. Similar local structure models can be expected for the crystalline compound **1-D₂O-CD₃OD** in our study. In this model, the CD₃ groups of the methanol and the water can be located in different cavities with close or distant mutual arrangement of intercalates.

To complete the discussion of the local structural models in Figures 1 and 8, it should be emphasized again that isotopic exchange (2), potentially involving the acidic protons of the phosphate groups was not detected experimentally or a content of DPO₄ groups due to this exchange is small as $\leq 4\%$. This result is surprising because generally the water-containing zirconium phosphates manifest a proton conductivity.^[30-33] According to the literature, the H⁺ transport in such zirconium phosphates can only occur under the following conditions:^[39,40] (a) the close proximity of the water molecules which are *firmly held but able to fully rotate* and (b) a strong hydrogen-bonding network on zirconium phosphate surface formed by water and phosphate groups which provide protons for donation. As seen in Figures 1 and 8, the dynamic/bonding modes of the intercalates do not meet these conditions and therefore, the isotope exchange is not significant (if it is generally present). In addition, as we assume, the hydrogen-bonding network shown in Figure 1 may even prevent from the isotopic exchange at preparations of the compounds presented in the present work. In fact, according to the literature,^[41] α -Zr(DPO₄)₂·nD₂O can be

prepared by titrating $\alpha\text{-Zr}(\text{HPO}_4)_2 \cdot \text{H}_2\text{O}$ with NaOH and then by back-titrating the product with DCl but not by a simple soaking with D_2O and the corresponding isotopic exchange. This practice supports well our conclusions.

4. CONCLUSIONS

Crystalline and amorphous α -zirconium phosphates, intercalated with D_2O and CD_3OD and also anhydrous zirconium phosphates have been comprehensively characterized by solid-state MAS NMR experiments on ^2H , ^1H , ^{31}P and ^{13}C nuclei. These experiments included ^1H and ^{31}P T_1 time measurements and the study of the kinetic proton-phosphorus cross-polarization. The $^{31}\text{P}\{^1\text{H}\}$ MAS NMR spectra of compounds **1-D₂O-CD₃OD** and **1-CD₃OD** have shown three types of HPO_4 groups: two of which were shown to be neighbors to water and methanol molecules. All the phosphate groups have been characterized by equal cross-polarization constants $T(\text{P-H})$, which do not feel the presence of deuterons in these groups. The $T_{1p}(^1\text{H})$ times in the rotating coordinate system, measured for crystalline and amorphous compounds **1-D₂O-CD₃OD**, **1-CD₃OD**, **1-An**, and **1-An-Am** are associated with a proton transfer and the fast proton-proton exchanges between the phosphate groups leading to their spectroscopic equivalency in the ^1H MAS NMR spectra. The proton-proton exchange most likely occurs via hydrogen bonds formed by these groups. The ^{31}P T_1 times measured for crystalline and amorphous zirconium phosphates have shown that the intercalated species do not affect the high-frequency mobility of the structurally-different phosphate groups. All the NMR experiments did not reveal a remarkable presence of DPO_4 groups

in the investigated compounds. According to the ^{31}P T_1 measurements, the DPO_4 content is estimated as $\leq 4\%$.

In contrast to the mobile water detected in compound **1-D₂O**,^[17] the ^2H solid-echo MAS NMR spectra of the zirconium phosphate **1-CD₃OD** intercalated by methanol have shown the presence of immobile methanol molecules. At the same time, these molecules maintain free CD_3 rotation around the C_3 -axis. The deuterium quadrupolar coupling constants, characterizing CD_3OD agree well with this conclusion: $\text{DQCC} = 47 \pm 3$ kHz for the CD_3 resonance at $\delta(\text{iso})$ of 4.3 ppm) and $\text{DQCC} = 195 \pm 7$ kHz for the resonance of the hydrogen bonded OD group, detected at $\delta(\text{iso})$ of 8.6 ppm. The corresponding structural model which satisfies all the experimental data has been suggested. In this model, the immobile methanol is hydrogen bonded to the zirconium-coordinated oxygen and is located in the cavity between two neighboring layers of the zirconium phosphate.

SUPPORTING INFORMATION

Additional supporting information may be found online in the Supporting Information section at the end of this article.

ACKNOWLEDGMENT

This work is supported by the U.S. Department of Energy (DOE), Basic Energy Sciences, Grant DE-SC0017864, for which grateful acknowledgment is made. We acknowledge the X-ray Diffraction Laboratory at Texas A&M University. H.-C.Z. acknowledges support from the Robert A. Welch Foundation (A-0030). We also thank Dr. V. V. Grushin for useful discussion.

ORCID

Vladimir I. Bakhmutov <https://orcid.org/0000-0002-5011-0385>

REFERENCES.

- [1] H. Nathan, B. Akhilesh, V. K. Challa, *Layered α -Zirconium Phosphates and Phosphonates*, in *Handbook of Layered Materials*, CRC Press, Boca Raton, USA, **2004**.
- [2] C. Ferragina, R. Di Rocco, P. Giannoccaro, P. Patrono, L. Petrilli, *J. Incl. Phenom. Macro.* **2009**, *63*, 1.
- [3] M. E. B. Santiago, M. M. Vélez, S. Borrero, A. Díaz, C. A. Casillas, C. Hofmann, A. R. Guadalupe, J. L. Colón, *Electroanalysis*. **2006**, *18*, 559.
- [4] A. Díaz, V. Saxena, J. Gonzalez, A. David, B. Casanas, C. Carpenter, J. D. Batteas, J. L. Colón, A. Clearfield, M. Delwar Hussain, *Chem. Commun.* **2012**, *48*, 1754.
- [5] A. Díaz, M. L. Gonzalez, R. J. Pérez, A. David, A. Mukherjee, A. Baez, A. Clearfield, J. L. Colón, *Nanoscale* **2013**, *5*, 11456.
- [6] A. Díaz, A. David, R. Pérez, M. L. González, A. Báez, S. E. Wark, P. Zhang, A. Clearfield, J. L. Colón, *Biomacromolecules*, **2010**, *11*, 2465.
- [7] H. Nakayama, *Phosphorus Research Bulletin*, **2009**, *23*, 1.
- [8] J. L. Colón, B. Casañas, *Drug Carriers Based on Zirconium Phosphate Nanoparticles*, in *Tailored Organic–Inorganic Materials*, John Wiley & Sons, Inc, Hoboken, NJ, **2015**, p. 395.
- [9] A. Contreras-Ramirez, S. Tao, G. S. Day, V. I. Bakhmutov, S. J. L. Billinge, H. C. Zhou, *Inorg. Chem.* **2019**, *58*, 14260.

- [10] C. Roiland, F. Fayon, P. Simon, D. Massiot *Journal of Non-Crystalline Solids*, **2011**, 357, 1636.
- [11] C. M. Morais, V. Montouillout, M. Deschamps, D. Iuga, F. Fayon, F. A. A. Paz, J. Rocha, C. Fernandez, D. Massiot, *Magn. Reson. Chem.* **2009**, 47, 942.
- [12] V. I. Bakhmutov, Y. Kan, J. A. Sheikh, J. González-Villegas, J. L. Colón, A. Clearfield, *Magn. Reson. Chem.* **2017**, 55, 648.
- [13] Khudozhitkov, A. E.; Toktarev, A. V.; Arzumanov, S. S.; Gabrienko, A. A.; Kolokolov, D. I.; Stepanov, A. G.; *Chem.Eur.J.* **2019**,25,10808.
- [14] Fu, Y.; Guan, H.; Yin, J; Kong, X.; *Coordination Chemistry Reviews* **2021**, 427, 213563, 1-17.
- [15] Vladimir I. Bakhmutov, V. I.; *Chem. Rev.* **2011**, 111, 530.
- [16] Petrov, O.; Tosner, Z.; Csoregh, Kowalewski, J.; Sandstrom, D.; *J. Phys. Chem. A*, **2005**, 109, 4442.
- [17] V. I. Bakhmutov, A. Contreras-Ramirez, A. Banerjee, H. C. Zhou, *Magn.Reson.Chem.* <https://doi.org/10.1002/mrc.5225>
- [18] M. Pica, *Catalysts*, **2017**, 7, 190, 2.
- [19] M. V. Ramos-Garces, J. L. Colon, *Nanomaterials*, **2020**, 10, 822, 4.
- [20] S. Cheng, G. Z. Peng, A. Clearfield, *Ind. Eng. Chem. Prod. Res. Dev.*, **1984**, 23, 219.
- [21] D. J. MacLachlan, K. R. Morgan, *J. Phys. Chem.* **1992**, 96, 3458.
- [22] W. Kolodziejski, J. Klinowski, *Chem. Rev.* **2002**, 102, 613.

- [23] R. H. Newman, J. A. Hemmingson, *Holzforschung* **1990**, *44*, 351.
- [24] V. I. Bakhmutov, A. Clearfield, *J. Phys. Chem. C* **2017**, *121*, 550.
- [25] V. I. Bakhmutov, A. Clearfield, *J. Phys. Chem. C* **2016**, *120*, 19225.
- [26] K. L. Dawson, I. E. Farnan, B. R. Constantz, S. W. Young, *Invest. Radiol.* **1991**, *26*, 946.
- [27] X. Kong, Characterization of proton exchange membrane materials for fuel cells by solid state NMR. Ph.D. Thesis, Iowa State University: **2010**; pp 130–133.
- [28] T. Sparrman, L. Svenningsson, K. Sahlin-Sjovold, L. Nordstierna, G. Westman, D. Bernin, *Cellulose*, **2019**, *26*, 8993.
- [29] K. Okada, D. Hirai, S. Kumada, A. Kosugi, Y. Hayashi, Y. Onuki, *J. Pharmaceut. Sci.* **2019**, *108*, 451.
- [30] A. Donnadio, M. Nocchetti, F. Costantino, M. Taddei, M. Casciola, S. F. Lisboa, R. A. Vivani, *Inorg. Chem.* **2014**, *53*, 13220.
- [31] R. Thakkar, H. Patel, U. Chudasama, *Bull. Mater. Sci.*, **2007**, *30*, 205.
- [32] W. H. J. Hogarth, J. Diniz, D. J. C. Costa, J. Drennan, G. Q. Lu, *J. Mater. Chem.*, **2005**, *15*, 754.
- [33] T. Ogawa, H. Ushiyama, K. Yamashita, J. M. Lee, T. Yamaguchi, *Chem. Lett.* **2010**, *39*, 736.
- [34] B. Kumari, M. Brodrecht, H. Breitzke, M. Werner, B. Grunberg, H.-H. Limbach, S. Forg, E. P. Sanjon, B. Drossel, T. Gutmann, G. Buntkowsky, *J. Phys. Chem. C* **2018**, *122*, 19540.
- [35] A. Clearfield, *Chem. Rev.* **1988**, *88*, 125.
- [36] Z. Luzf, A. J. Vega, *J. Phys. Chem.* **1987**, *91*, 374.

- [37] A. Thursfield, M. W. Anderson, *J. Phys. Chem.* **1996**, *100*, 6698.
- [38] M. Hunger, T. Horvath, *J. Am. Chem. Soc.* **1996**, *118*, 12302.
- [39] E. Fabbri, D. Pergolesi, E. Traversa, *Chem. Soc. Rev.*, **2010**, *39*, 435.
- [40] R. Gloukhovski, V. Freger, Y. Tsur, *Rev. Chem. Eng.*, **2018**, *34*, 455.
- [41] A. L. Blumenfeld, A. S. Golub, G. Protsenko, Yu. N. Novikov, M. Casciola, U. Costantino, *Solid State Ionics* **1994**, *68*, 105.